This is a preprint, the final version is subject to change, of the American Mineralogist (MSA)
Cite as Authors (Year) Title. American Mineralogist, in press.
(DOI will not work until issue is live.) DOI: http://dx.doi.org/10.2138/am-2017-5850

Revision 2

Diamond, Moissanite and other unusual minerals in podiform chromitites from the Pozanti-Karsanti ophiolite, southern Turkey: implications for the deep mantle origin and ultra-reducing conditions in podiform chromitite.

DONGYANG LIAN[1,2], JINGSUI YANG[1*,2], YILDIRIM DILEK[2,3], WEIWEI WU[1,2], ZHONGMING ZHANG[2], FAHUI XIONG[2], FEI LIU[2] AND WENGDA ZHOU[1,2]

[1]Faculty of Earth Sciences, China University of Geosciences (Wuhan), Wuhan, 430074, China

[2]CARMA, Institute of Geology, Chinese Academy of Geological Sciences, Beijing, 100037, China

[3]Department of Geology and Environmental Earth Science, Miami University, Oxford, OH 45056, USA

Corresponding author at: 26 Baiwanzhuang Road, Beijing 100037, China. MP: +86 13701228542,

E-mail address: yangjsui@163.com (Jingsui Yang)

ABSTRACT

The Pozanti-Karsanti ophiolite situated in the eastern Tauride belt, southern Turkey, is a well preserved oceanic lithosphere remnants comprising, in ascending order, mantle peridotite, ultramafic and mafic cumulates, isotropic gabbros, sheeted dikes and basaltic pillow lavas. Two types of chromitites are observed in the Pozanti-Karsanti ophiolite. One type of chromitites occurs in the cumulate dunites around the Moho and the other type of chromitites is hosted by the mantle harzburgites below the Moho. The second type of chromitites has massive, nodular and disseminated textures. We have conducted the mineral separation work on the podiform chromitites hosted by harzburgites. So far, more than 200 grains of microdiamond and more than 100 grains of moissanite (SiC) have been separated from the podiform chromitite. These minerals have been identified by EDS

Always consult and cite the final, published document. See http:/www.minsocam.org or GeoscienceWorld

and Laser Raman analyses. The diamonds and moissanite are accompanied by large amounts of rutile. Besides, Zircon, monazite and sulphide are also very common phases within the separated minerals. The discovery of diamond, moissanite and the other unusual minerals from podiform chromitite of the Pozanti-Karsanti ophiolite provides new evidences for the common occurrences of these unusual minerals in ophiolitic peridotites and chromitites. This discovery also suggests that deep mantle processes and materials have been involved in the formation of podiform chromitite.

Keywords: ophiolite, chromitite, diamond, moissanite,

INTRODUCTION

Ophiolites represent remnants of ancient oceanic lithosphere that were tectonically emplaced onto the continents (Dilek and Furnes 2011; Pearce 2014; Whattam and Stern 2011). Podiform chromitites commonly occur in ophiolites of different ages and areas (González-Jiménez et al. 2014; Rollinson and Adetunji 2015; Yang et al. 2015; Zhang et al. 2016; Zhou et al. 2014). According to the chemical composition of chromite, chromitites can be classified into the high-Cr group (Cr#=Cr/ (Cr + Al) of the chromite >0.6) and high-Al group (Cr#<0.6) (Dickey 1975; Thayer 1970). Both high-Al and high-Cr chromitites may occur in the same ophiolite (Akmaz et al. 2014; González-Jiménez et al. 2011; Uysal et al. 2009). High-Cr chromitites are interpreted to form by the reaction between boninitic or arc-related magmas with the depleted harzburgite in the suprasubduction zone environment (Arai 1997; Uysal et al. 2007; Xiong et al. 2015; Zhou et al. 1996), whereas high-Al chromitites are suggested to crystallize in equilibrium with MORB-type melts in the mid-ocean ridge or back-arc environment in the subduction zone (Arai and Matsukage 1998; Pagé and Barnes 2009; Zhou et al. 2001, 2014). In general, previous genetic models all suggest that chromitites formed by melt-rock reaction, magma mingling and crystallization in the shallow depth (< 30km) and no deep processes or materials have

Always consult and cite the final, published document. See http:/www.minsocam.org or GeoscienceWorld

been involved.

The redox states of the earth's mantle have been established and suggested to be progressively reduced with increasing depth based on natural igneous rock samples and a series of experiments (Frost and McCammon 2008; Stagno et al. 2013). The upper part of the upper mantle where podiform chromitites are suggested to form, has oxygen fugacity within ± 2 log units of the fayalite-magnetite-quartz (FMQ) oxygen buffer (Frost and McCammon 2008). Recently, diamonds, moissanite and other unusual minerals have been recovered from peridotites and podiform chromitites (high-Cr and high-Al type) in ophiolites of different ages and orogenic belts (Howell et al. 2015; Robinson et al. 2015; Tian et al. 2015; Yang et al. 2015). As these minerals are mostly unexpected to be found in the chromitites and peridotites, people have questioned the factitious contamination origin of these minerals. However, in-situ diamonds (enclosed by OsIr alloy) (Yang et al. 2007), moissanite (enclosed by chromite) (Liang et al. 2014), coesite (rimming FeTi alloy) (Yang et al. 2007) and exsolution clinopyroxene lamellaes (in chromite) (Yamamoto et al. 2009) have been observed in chromitite of Luobusa ophiolite in China and Ray-Iz ophiolite in Russia. Thus, these unusual minerals are original rather than contaminated to the ophiolitic peridotites and podiform chromitites (Howell et al. 2015). Natural diamonds generally crystallize at depths exceeding ~150 km and temperatures above 950 ℃ at fO_2 conditions around iron-wüstite (IW) buffer in the upper mantle (Cartigny 2005; Jacob et al. 2004; Stagno et al. 2015; Stagno and Frost 2010) and occasionally in the lower mantle (Kaminsky et al. 2009; Stachel et al. 2005). The in-situ diamond in the OsIr alloy separated from Luobusa chromitite suggests pressures > 4 GPa (depth of > 120 km), while the coesite-kyanite intergrowth around a FeTi alloy indicate a potential pressure > 9 GPa (depth of > 280 km) (Yang et al., 2007). High-pressure nitrides including TiN and c-BN, oxides and metals have also been recovered within the coesites riming a FeTi alloy of the Luobusa chromitites (Dobrzhinetskaya et al., 2009; Galuskin et al., 2013). These mineral inclusions in the coesite record a high pressure and temperature conditions and very low fo_2 which indicates the formation depth of > 300 km (pressure > 10 GPa) (Dobrzhinetskaya et al., 2009). Coesites and exsolution clinopyroxene lamellaes in the chromite also suggest an ultrahigh-pressure origin of at least 100 km, maybe more than 300 km deep for the Luobusa chromitites (Yamamoto et al. 2009). Based on thermodynamic calculation and experiments results, it is generally accepted that moissanite forms at extremely reducing conditions with the oxygen fugacity at least five to six log units below IW (Mathez et al. 1995; Schmidt et al. 2014; Ulmer et al. 1998). Thus, the ultra-high pressure (UHP) and ultra-highly reduced (UHR) conditions indicated by diamond, moissanite and other unusual minerals have put challenges to the traditional genetic models for ophiolites and chromitites.

As this mineral separation work has only been conducted on limited ophiolites, we are still unclear whether these unusual minerals have a common occurrence in the worldwide ophiolites. For better understanding of this problem, we have collected podiform chromitite hosted by harzburgite from the Pozanti-Karsanti ophiolite (PKO) (or the Aladag ophiolite). Mineral separation work has been carried out on these chromitites. In this paper, we document the characteristics of podiform chromitite and unusual minerals from this chromitite, in order to contribute to the understanding of the origin of ophiolite and podiform chromitite.

BACKGROUND: GEOLOGICAL SETTING

The NE-SW trending PKO is located in the eastern Tauride belt, southern Turkey (Fig. 1) (Parlak et al. 2002; Saka et al. 2014). The Tauride belt mainly consists of Paleozoic and Early Mesozoic platform carbonates, Paleozoic and early Mesozoic volcanosedimentary and epiclastic rocks,

Always consult and cite the final, published document. See http:/www.minsocam.org or GeoscienceWorld

This is a preprint, the final version is subject to change, of the American Mineralogist (MSA)
Cite as Authors (Year) Title. American Mineralogist, in press.
(DOI will not work until issue is live.) DOI: http://dx.doi.org/10.2138/am-2017-5850

Cretaceous ophiolite complexes and late Cretaceous and younger post-collisional sedimentary and volcanic rocks (Dilek et al. 1999).

The PKO in the Aladag region is offset from the Mersin ophiolite by the sinistral Ecemis fault (Fig. 1). An imbricated stack of thrust sheets resting on the Taurus allochthon can be observed in Aladag region (Fig. 2) (Polat and Casey 1995). From the bottom to the top, the thrust sheets over the carbonate platform consist of the Aladag mélange, the metamorphic sole and the PKO (Lytwyn and Casey 1995; Parlak et al. 2002; Polat and Casey 1995; Saka et al. 2014). The metamorphic sole and the Aladag mélange were accreted to the base of the PKO during intra-oceanic subduction, transportation and final obduction of the ophiolite onto the Menderes-Taurus block (Çelik et al. 2006; Dilek et al. 1999; Polat et al. 1996).

The Aladag mélange is composed of sedimentary, igneous and metamorphic blocks with serpentinitic to politic matrix and can be divided into the upper tectonic slice, the middle tectonic slice and the lower tectonic slice (Polat and Casey 1995; Tekeli et al. 1983). Geochemical studies demonstrate that materials from this mélange were derived from both the oceanic and continental sources (Polat et al. 1996). Metamorphic sole overlying the Aladag mélange has a typical inverted metamorphic sequence (Polat and Casey 1995). This dynamothermal metamorphic sole consists of greenschist rocks at the bottom and amphibolite facies rocks on the top. The intra-oceanic subduction of the Neo-Tethyan Ocean happened around 90-94 Ma, as indicated by the K-Ar age of the amphibolite facies rock in the metamorphic sole (Çelik et al. 2006; Dilek et al. 1999; Thuizat et al. 1981). The PKO is a well preserved oceanic lithosphere remnants comprising, in ascending order, mantle peridotites (Fig. 3a), ultramafic and mafic cumulates (Fig. 3b), isotropic gabbros, sheeted dikes and basaltic pillow lavas (see Supplementary. 1) (Parlak et al. 2000, 2002; Saka et al. 2014).

Always consult and cite the final, published document. See http:/www.minsocam.org or GeoscienceWorld

PETROGRAPHY

Peridotites

Peridotites from the PKO are dominated by harzburgites with subsidiary dunites (Fig. 3a). These peridotites are variably serpentinized. Harzburgite samples contain 75-80 modal% olivine, 15-20 modal% orthopyroxene, 1-2 modal% clinopyroxene and 1-2 modal% chromite (Fig. 4a, 4b). Dunites hosted by harzburgites are strongly serpentinized and contain 97-98 modal% olivine and 2-3 modal% chromite in original modal mineralogy (Fig. 4c). Olivines in harzburgites are generally subhedral and 1-3mm across. Olivines are cut through by networks of serpentines and magnetites. Orthopyroxenes ranging from 0.3 to 5 mm along their long axes are occasionally serpentinized to bastite. Some orthopyroxene grains have lobate boundaries with small olivine or clinopyroxene grains filling up the embayments. Clinopyroxenes in harzburgites are generally anhedral, 0.1-0.5 mm across and occur either as interstitial grains or as inclusions in orthopyroxenes. Inclusions of olivine and chromite are also occasionally observed in orthopyroxenes. Chromites in the harzburgites are reddish brown, subhedral to anhedral ranging from 0.1mm to o.5mm, while chromites in dunites are nearly opaque, black, anhedral and 0.1-0.7 mm across (Fig. 4a, 4c). Chromites in dunites generally have an alteration rim. Olivines sometimes occur as inclusions in the chromites (Fig. 4b).

Chromitites

Chromitites occur in two different horizons of the PKO. One type of chromitites occurs in cumulate dunites around the Moho (Fig. 3b), while the other one occurs in harzburgites below the Moho (Fig. 3c, 3d). Both types of chromitite are strongly altered. Cumulate chromitites and the hosted cumulate dunites are transitional to each other with no distinct boundary. This type of chromitites has massive or disseminated textures (see Supplementary. 2). Chromite grains in disseminated chromitites

Always consult and cite the final, published document. See http:/www.minsocam.org or GeoscienceWorld

are generally euhedral to subhedral, 0.2-2mm across and black in color. Relicts of fresh olivine grains can be observed occasionally. Chromitites hosted by harzburgites generally have thin dunitic envelopes and show massive or nodular textures, which is typical for podiform chromitites (Fig. 3c, 3d, 4d). Original silicate minerals in the podiform chromitites are altered into serpentine, chlorite or clay minerals. Olivine and clinopyroxene inclusions can be observed in the chromitites (Fig. 4e, 4f). The chromite nodules ranging from 3 mm to 10 mm are dominated by chromites with minor alteration minerals filling the fissures (Fig. 3c). Massive chromitites in the harzburgites consist of over 95% percent of chromites with minor alteration minerals including serpentines and chlorites.

SAMPLING AND ANALYTICAL METHODS

About 500 kg of podiform chromitites hosted by the PKO harzburgites were collected. Preliminary mineral separation work was carried out at the Institute of Multipurpose of Utilization of Mineral Resources, Chinese Academy of Geological Sciences, Zhengzhou. The detailed mineral separation procedure has been described by Xu et al. (2009). Before conducting the experiments, all of the equipments were carefully cleaned. Cares have been taken during all the procedures to avoid contamination.

After the preliminary mineral separation work, the unusual minerals were carefully selected under the binocular eyepiece. The selected mineral grains are analyzed by the Nova Nanosem 450 scanning electron microscope with an energy-dispersive spectrometer (EDS) and a RENISHAW-1000 Laser Raman in the State Key Laboratory for Continental Tectonics and Dynamics. The operating conditions for SEM were set at 20 kV and beam current is 15 nA. Cobalt metal was applied to calibration procedure of the peak position on the energy scale to allow semi-quantitative analyses. Minerals in the harzburgites and chromitites from the PKO were analyzed by a JEOL JXA-8100 electron microprobe at

Always consult and cite the final, published document. See http:/www.minsocam.org or GeoscienceWorld

This is a preprint, the final version is subject to change, of the American Mineralogist (MSA)
Cite as Authors (Year) Title. American Mineralogist, in press.
(DOI will not work until issue is live.) DOI: http://dx.doi.org/10.2138/am-2017-5850

the state Key laboratory for Continental Tectonics and Dynamics, Institute of Geology, Chinese Academy of Geological Sciences, Beijing. The measurements were performed using wavelength dispersive spectrometers at 15 kV and 20 nA with a beam diameter of 5μm. Natural and synthetic standards were used for calibration. The uncertainty of the electron probe microanalysis are within ±1% for the major elements. The amount of Fe^{3+} in the chromite was calculated assuming the ideal chromian spinel stoichiometry of $A^{2+}B^{3+}{}_2O_4$.

RESULTS

Mineral chemistry of harzburgites and chromitites

Mineral chemistry results of harzburgites and chromitites from the PKO are listed in Supplementary. 3. Olivine in harzburgites has normal Fo (Fo = $100*Mg^{2+} / (Mg^{2+} + Fe^{2+})$) contents ranging between 91.0 and 93.2. One euhedral olivine inclusion enclosed in chromite from podiform chromitite has been analyzed (Fig. 4e). The result turned out that this olivine grain has quite higher Fo content (Fo = 97.1) compared to those of olivines in harzburgites (Fig. 5a). Orthopyroxene (Opx) in harzburgites has $Mg^{\#}$ values ($Mg^{\#} = 100*Mg^{2+} / (Mg^{2+} + Fe^{total})$) around 91.5 and clinopyroxene (Cpx) has $Mg^{\#}$ values around 94.5. Two euhedral clinopyroxene inclusions hosted by chromite in chromitite have relatively higher $Mg^{\#}$ values of 96 (Fig. 4f). Ferrian chromite and magnetite may occur along the rims and cracks of chromite grains, but only the unaltered cores of chromite grains were analyzed. Chromites from PKO harzburgites and chromitites are classified as aluminum chromites (Stevens 1944) and fall in the field of Turkish chromitites (Ucurum et al. 2006) (Fig. 5b). Chromites in harzburgites have $Cr^{\#}$ values ranging from 61.0 to 64.2 and quite low TiO_2 contents and chromites in the podiform chromitites have $Cr^{\#}$ values ranging from 76.8 to 79.1 (Fig. 5c-5f).

Unusual minerals recovered from the podiform chromitites

Always consult and cite the final, published document. See http:/www.minsocam.org or GeoscienceWorld

Diamond

We have separated more than one hundred grains of diamond from the PKO podiform chromitites (Fig. 6). The diamonds are generally transparent, colorless to pale yellow and tiny (ca. 50-250 μm). They are generally irregular fragments, with a few of them showing subhedral to euhedral shape (Fig 6b). As shown in the SEM images, most diamonds have sharp edges (Fig. 6a, 6b), whereas some of them are rounded (Fig. 6d). Raman shifts of the analyzed diamonds are all around 1334 cm^{-1} (Fig. 6c).

Moissanite

Moissanite crystals recovered from the chromitites are transparent, usually occurring as irregular flakes or fragments with a size of 50-300 μm (Fig. 7). Moissanite generally has different colors, including blue, light green to green, and colorless. The analyzed moissanite crystals have Raman shifts around 766 cm^{-1}, 786 cm^{-1} and 968 cm^{-1} (Fig. 7c). Some of the green moissanite show polycrystalline crystals (Fig. 7e). Energy-dispersive spectroscopy analyses confirm that moissanite are mainly composed of C and silicon (Fig. 7f).

Silicate of octahedral pseudomorph

More than one hundred grains of silicate showing perfect octahedral pseudomorphs have been separated from the PKO chromitites (Fig. 8). These grains are sub-transparent to transparent, light purple, 60-400 μm across euhedral crystals, with octahedral forms (Fig. 8a-8c). Several grains of octahedral pseudomorphs are light yellow, subtransparent to transparent and 100-350 μm across. Due to incompletely separation, relicts of chromite can be observed being bonded to these octahedral pseudomorphs indicating that these octahedral pseudomorphs are protogenous in the chromitite rather than contaminated (Fig. 8c). SEM images of the surfaces of these silicates show that these minerals are composed of very fine rounded grains (Fig. 8d). Energy-dispersive spectroscopy analyses suggest that

Always consult and cite the final, published document. See http:/www.minsocam.org or GeoscienceWorld

these silicates of octahedral pseudomorph have two different compositions. One type of these silicate pseudomorphs is composed of Mg, Si, Al, Cr, Fe, and O elements (Fig. 8e), whereas the other type consists of Mg, Si and O with no Al and Cr elements (Fig. 8f).

Other minerals

In addition to the above-mentioned minerals, other minerals including oxides (hematite, magnetite, rutile and quartz), sulfides, silicates (magnesian olivine, pyroxene, spessartite, Zircon, chlorite and serpentine) and monazites have also been recovered (Fig. 9). Zircons from the chromitites are generally prismatic and subhedral to rounded with different colors (Fig. 9a, 9b). Mineral inclusions can be observed in the zircons. About ten grains of monazites have been recovered from the chromitites (Fig. 9d, 9). These monazites are light yellow, inclusion-bearing and around 100 μm across. Hundreds of rutiles have also been separated from the chromitites. These rutiles are brown to reddish brown, 50-200 μm, subhedral to anhedral and inclusion-bearing (Fig. 9g, 9h).

DISCUSSION

Characteristics of harzburgite and chromitite

The PKO harzburgites have quite low clinopyroxene contents indicating a relatively high degree of partial melting. Forsterite content of olivine grains combining with $Cr^{\#}$ value of coexisting chromites in the peridotites is also a useful indicator of partial melting degree and tectonic setting (Arai 1994; Parkinson and Pearce 1998; Yang et al. 2015). In the $Cr^{\#}$ vs. Fo diagram, all our samples plot within the olivine-spinel mantle array (OSMA) demonstrating that the harzburgites are melting residues rather than cumulate rocks (Arai 1994) (Fig. 5a). The high $Cr^{\#}$ values of chromites in harzburgites suggest a quite high degree of partial melting, which is consistent with the depleted modal mineralogy of the harzburgites (Fig. 5a). All of the harzburgites fall in the SSZ peridotites field in the $Cr^{\#}$ vs. Fo diagram

Always consult and cite the final, published document. See http:/www.minsocam.org or GeoscienceWorld

indicating that the Pozanti-Karsanti harzburgites formed in the suprasubduction zone environment (Fig. 5a).

The primary core compositions of chromites are also plotted in other diagrams to determine the tectonic setting of the harzburgites and the type of chromitite in the harzburgites (Fig. 5c-5f). In the $Mg^{\#}$ vs. $Cr^{\#}$ diagram, chromites in harzburgites plot in the field of forearc peridotites, while those in chromitite plot out of both the abyssal and forearc peridotite fields (Fig. 5c). In the TiO_2 vs. $Cr^{\#}$ diagram (Fig. 5d), chromites from harzburgites also fall in the field of forearc peridotites and plot to the end of the melting trend suggesting a quite depleted nature of the harzburgites. Chromitite plots close to the melt-rock reaction trend from depleted peridotite to boninitic or arc-related magma (Fig. 5d), which indicates a melt-rock reaction origin for podiform chromitite (Arai and Matsukage 1998; Zhou et al. 1998). The PKO chromitite differs from stratiform chromitite both structurally and geochemically. Chromitite chosen for mineral separation work has nodular texture, which is typical for podiform chromitite (Thayer 1964). In the Cr_2O_3 vs. Al_2O_3 diagram, chromites from harzburgites fall in the field of forearc peridotites and those of chromitite plot in the field of podiform chromitite (Fig. 5e). In the Cr_2O_3 vs. TiO_2 diagram, chromites from PKO chromitite plot below the boundary of stratiform and podiform chromitites. Compared to the chromite in stratiform chromitites, those from podiform chromitite have relatively lower TiO_2 contents (Fig. 5f). The modal mineralogy and mineral chemistry suggest that harzburgites from the PKO experienced relatively high degree of partial melting in the suprasubduction zone environment. Geochemical and structural evidences demonstrate that chromitite hosted by harzburgites in PKO is typical high-Cr podiform chromitite.

Discovery of unusual minerals in PKO and its significance

Diamond, moissanite, silicates of octahedral pseudomorph and other crustal minerals have been

Always consult and cite the final, published document. See http:/www.minsocam.org or GeoscienceWorld

This is a preprint, the final version is subject to change, of the American Mineralogist (MSA)
Cite as Authors (Year) Title. American Mineralogist, in press.
(DOI will not work until issue is live.) DOI: http://dx.doi.org/10.2138/am-2017-5850

recovered from the podiform chromitite in the PKO. As these minerals are unexpected in chromitites and peridotites, these discoveries were firstly thought to be disputable. However, in-situ diamonds have been observed in both the Luobusa and Ray-Iz chromitites (Yang et al. 2007, 2015). In-situ diamonds from podiform chromitites show two different occurrences, including (1) 1μm across inclusion in an OsIr alloy separated from Luobusa chromitite (Yang et al. 2007); and (2) 300 μm across diamond enclosed by chromite from the Luobusa and Ray-Iz chromitites (Yang et al. 2014, 2015). Different scientific groups have reported to have recovered diamonds, moissanite and other "crustal" minerals from podiform chromitites of different ophiolites in different labs (Griffin et al. 2016; Howell et al. 2015; McGowan et al. 2015; Trumbull et al. 2009). Thus, these minerals are intrinsic to the ophiolitic peridotites and podiform chromitites rather than introduced by artificial contamination.

Natural occurrences of diamond are manifold but mainly fall into three categories, including (1) volcanic rocks (kimberlites, lamproites and lamprophyres) from the sub-continental lithosphere, (2) ultra-high-pressure metamorphic rocks exhumed by the orogenic process of continental collision, and (3) meteorites and impact-related rocks (Cartigny 2005; Shirey et al. 2013; Yang et al. 2014). A new occurrence of diamond called "ophiolitic diamond" was reported to be found both in mineral concentrates and as inclusions hosted by chromites in peridotites and chromitites from ophiolites in Xinjiang (Tian et al. 2015), Tibet (Xu et al. 2015) and Inner Mongolia (Zhu et al. 2015) provinces of China, Myitkyina ophiolite of Myanmar (Yang et al. 2014) and Ray-Iz (Yang et al. 2015) ophiolite of Russia. Despite of the different occurrences, diamonds only crystallize at high pressures (> 4.5 GPa) and temperatures (> 950 ℃) (Cartigny 2005). Diamonds in the mantle and metamorphic rocks are widely accepted to form from C-O-H bearing fluids or melts with the oxygen fugacity below the Enstatite-Magnesite-Forsterite-Graphite/Diamond (EMOG/EMOD) buffer (Stachel and Luth 2015;

Always consult and cite the final, published document. See http:/www.minsocam.org or GeoscienceWorld

Stagno and Frost 2010). Thus, discovery of diamonds suggests that ultra-high pressure processes or materials have involved in the formation of the PKO podiform chromitite.

Natural moissanite also occurs in a variety of extraterrestrial and terrestrial rocks, including meteorites (Alexander 1993; Moissan and Siemens 1904); kimberlites ((Leung et al. 1990; Mathez et al. 1995; Shiryaev et al. 2011); serpentinites (Xu et al. 2008); peridotites and related podiform chromitites (Trumbull et al. 2009; Yang et al. 2015). Based on the thermodynamic calculation, Mathez et al. (1995) concluded that moissanite is only stable in the upper mantle with the oxygen fugacity five to six log units below the IW buffer. Schmidt et al. (2015) synthesized moissanite in a graphite-silicate system with fo_2 conditions 5-6.5 log units below the IW buffer at 2-10 GPa and 1500-1700 ℃, which is consistent with the previous calculations (Mathez et al. 1995). Golubkova et al. (2016) computed phase diagrams sections for the alloys, carbides and Fe-silicides and concluded that Moissanites can only occurs at oxygen fugacities 6.5-7.5 log units below the IW buffer. Metallic Si is a very common inclusion in moissanite both from kimberlites and podiform chromitite (Shiryaev et al. 2011; Trumbull et al. 2009), which has also been observed in moissanite recovered from the PKO chromitites. Experiments indicate that the formation of metallic Si require the environment to have oxygen fugacity 3-5 log units below that of SiC-forming reaction (Golubkova et al. 2016; Schmidt et al. 2014). Hereby, Moissanites recovered from the PKO chromitite imply a super-reduced condition.

Several dozens of silicates with perfect octahedral morphology have been separated from podiform chromitites. These octahedral silicates have also been separated from the Luobusa chromitites (Griffin et al. 2016; Robinson et al. 2004), whereas no such minerals have been reported in the Ray-Iz, Hegenshan and Sartohay chromitites. These octahedral grains are composed of clinochlore, lizardite or antigorite (Griffin et al. 2016). Several transparent grains of these octahedral silicates from Luobusa

Always consult and cite the final, published document. See http:/www.minsocam.org or GeoscienceWorld

chromitite are anhydrous and have cubic structures analogous to those of ringwoodite. The hydrous octahedral silicates are suggested to be altered from a high-pressure form of olivine, possibly ringwoodite (Robinson et al. 2004). The transformation depth of wadsleyite to ringwoodite is at ~520 km (Frost 2008; Ghosh et al. 2013; Ringwood 1975). The existence of these octahedral silicates may also indicate a deep origin of the PKO chromitites.

Other minerals recovered from the Pozanti-Karsanti chromitites mainly include zircons, rutiles, and monazites. Zircons have been reported to be both in peridotites and chromitites of different locations (Akbulut et al. 2016; McGowan et al. 2015; Yamamoto et al. 2013; Yang et al. 2015; Zheng et al. 2006). Nine zircons from podiform chromitite in SW Turkey are interpreted to originate from metamorphism or ocean crust recycled during subduction (Akbulut et al. 2016). Zircons in the Luobusa chromitite contain two different groups: One group of zircons is generally rounded and subhedral to anhedral with a wide age range from the Cretaceous to Late Archean (Robinson et al. 2015; Yamamoto et al. 2013); the other group of zircons is euhedral with distinct, narrow oscillatory zoning (McGowan et al. 2015). The first group of zircons was suggested to originate from crustal materials that have been subducted into the mantle, and the second group of zircons crystallized from boninitic magmas during the crystallization of chromite grains in the suprasubduction zone environment (McGowan et al. 2015). Zircons from the PKO chromitites show different colors (brown to colorless) and shapes (anhedral to euhedral), which indicate different origin of these zircons (Robinson et al. 2015; Yang et al. 2015; Zhou et al. 2014).

The discovery of diamond, moissanite, octahedral silicates and other “crustal” minerals in the chromitites imply that these chromitites from the PKO may not simply form by melt-rock interaction and magma mingling in the shallow depth. Deep mantle materials or processes and assimilation of deep

Always consult and cite the final, published document. See http:/www.minsocam.org or GeoscienceWorld

subducted crustal materials have taken part in the formation of podiform chromitites.

IMPLICATIONS

Both high-Al and high-Cr podiform chromitites are widely distributed in Turkish ophiolites and have been generally interpreted to form through melt-rock reaction in the supra-subduction setting (Akbulut et al. 2016; Akmaz et al. 2014; Caran et al. 2010; Uysal et al. 2009). However, the ultra-reduced and/or ultra-high-pressure conditions indicated by the unusual minerals recovered from PKO chromitite have impelled us to reconsider the traditional formation models of Turkish podiform chromitite.

Several models have been proposed for the occurrence of diamond, moissanite and other unusual mineral in the Luobusa podiform chromitite. These models can be classified into two groups including the plume-related model (Xiong et al. 2015; Xu et al. 2015; Yang et al. 2015) and deep-subduction model (Griffin et al. 2016; McGowan et al. 2015; Robinson et al. 2015; Zhou et al. 2014). In the plume-related model, diamonds, moissanite and other UHP minerals have been suggested to form in the deep upper mantle or the transition zone and were brought up into the upper mantle by plume. However, Howell et al. (2015) pointed out that diamonds from Luobusa chromitite are distinct from natural "superdeep" diamonds. The unaggregated nitrogen, combined with the lack of evidence for resorption or plastic deformation indicate "ophiolitic diamonds" have a short residence in the mantle. Therefore, "ophiolitic" diamond was not likely to form in the mantle transition zone and stay in the mantle for a long period. Moissanite from chromitite has been suggested to form in the lower mantle or the core-mantle boundary based on the ultra-highly reduced conditions needed for the formation of moissanites (Mathez et al. 1995; Trumbull et al. 2009; Yang et al. 2015). Under these highly-reduced conditions, silicates coexisting with SiC should be Fe-Free and thus have unusually high $Mg^{\#}$ values

Always consult and cite the final, published document. See http:/www.minsocam.org or GeoscienceWorld

(Schmidt et al. 2014). Olivines in harzburgite have Fo contents around 92.0, Opx and Cpx have Mg# values around 91.0 and 94.0, respectively, indicating disequilibrium between the mantle phases with SiC and such super-reduced environment cannot exist in large-scale in the mantle. Frost and McCammon (2008) pointed out that the fo_2 of the lower mantle only fall in a narrow range between IW and IW -1.5 and oxygen fugacity of several log units below IW buffer is not achieved anywhere in the mantle. Besides, as calculated by Schmidt et al. (2014), SiC grains of 1mm would react with the Fe-component of silicate minerals to form iron carbide or metal and be exhausted within <1Ma at temperatures above 800℃. Schmidt et al. (2014) and Golubkova et al. (2016) concluded that SiC from podiform chromitites forms through a relatively low-temperature process (< 700-800℃) in a grain-scale micro-environment. Considering the high temperature and the oxygen fugacities of the lower mantle, it seems that the lower mantle was not an ideal formation place for moissanite (Golubkova et al. 2016; Schmidt et al. 2014). Temperatures of the Moho overlying the subducting slab in the suprasubduction zone have temperatures around 700 ℃(Bostock et al. 2002; Parkinson and Pearce 1998; Ueda et al. 2008). However, the suprasubduction zone has oxygen fugacities generally between FMQ (fayalite-magnetite-quartz) -1.1 (log units) and FMQ + 1.8 (Parkinson and Pearce 1998), which is also too oxidized for the formation of moissanite. Schmidt et al. (2014) suggested fluid percolation in the mantle and crystallization of hydrous phases can result in super reduced micro-environments, which thus lead to the formation of SiC on grain boundary without equilibration with the bulk rock on a larger scale. Thus, the moissanite from podiform chromitite may have crystalized in the mantle peridotite in the suprasubduction zone.

Ophiolitic units including mantle peridotite, ultramafic-mafic cumulate, isotropic gabbro and mafic dikes of the PKO have also been well studied (Lytwyn and Casey 1995; Parlak et al. 2002; Polat

Always consult and cite the final, published document. See http:/www.minsocam.org or GeoscienceWorld

and Casey 1995; Saka et al. 2014). Although Saka et al. (2014) suggested that PKO peridotites initially formed in the mid-ocean ridge (MOR) environment and then further depleted in the suprasubduction-zone (SSZ) environment, it should be noted that these peridotites show chemical characteristics more consistent with SSZ peridotites (Saka et al. 2014). Ultramafic cumulates in the PKO were suggested to crystalize from primary basaltic melts at medium to high-pressure conditions in the subduction zone (Parlak et al. 2002). Mineral and whole-rock geochemistry of mafic cumulate rocks and isotopic gabbros from the PKO suggest that these rocks formed from a melt that was produced by melting of depleted source in an intra-oceanic suprasubduction zone tectonic setting (Parlak et al. 2000; Saka et al. 2014). Mafic to intermediate dikes intruding the metamorphic sole and the ophiolitic sequences have geochemical characteristic similar to island-arc basalts and basaltic andesites (Lytwyn and Casey 1995). Thus, the PKO ophiolite shows great affinity to the SSZ-type ophiolite, and a two stages of evolution process, namely from the MOR to the SSZ environment, may not be necessary for the PKO. Whattam and Stern (2011) establish the "subduction initiation rule" and predict that most ophiolites form during subduction initiation (SI). We conclude that the PKO may also have formed during subduction initiation and podiform chromitite formed later after the depletion of mantle peridotites.

Here, based on previous study and our new work, we proposed a three-stage model for the origin of the Pozanti-Karsanti ophiolite, podiform chromitite and these unusual minerals.

(a) During the initial closure of the Neo-Tethys Ocean in southern Turkey, slab sinking and incipient trench rollback result in the upwelling of fertile asthenosphere into the space over the subducting slab following the "subduction initiation rule" (Stern 2004; Stern et al. 2012; Whattam and Stern 2011). Decompression partial melting of the asthenosphere mantle generated MORB-type magmas

Always consult and cite the final, published document. See http:/www.minsocam.org or GeoscienceWorld

and the PKO ultramafic cumulate rocks have crystallized from such primary basaltic melts (Parlak et al. 2002) . Addition of slab-derived fluids into the overlying mantle resulted in further melting of the already depleted mantle, which produced melts for the formation of mafic cumulates and isotropic gabbros in the PKO (Parlak et al. 2000; Saka et al. 2014). Mantle peridotites in the PKO have experienced ~24% to 30% partial melting and enriched by the fluids released from the subducting slab in the SSZ tectonic setting (Saka et al. 2014).

(b) With continuing subduction, the downgoing slab become dehydrated and experienced greenschist, amphibolite and eclogite facies metamorphism. Slab-derived fluids move upward into the mantle wedge and mantle peridotite are strongly serpentinized/altered. Fluids percolation, crystallization of hydrous minerals and other processes in the mantle wedge may create micro-super-reduced environment, which will result in the crystallization of SiC below the Moho in the mantle wedge (Golubkova et al. 2016; Schmidt et al. 2014). The subducting slab break off at ca. 120-160 km due to the development of dense metamorphic rocks (mainly eclogites), and diamonds may form at this depth. The breaking-off of subducting slab creates a slab window for the upwelling of underlying asthenosphere. Silicon-rich magma produced by the decompression melting of upwelling asthenosphere may contain coesite, inferred ringwoodite (octahedral silicate), and UHP chromite with inferred CF structure (Robinson et al. 2015; Yang et al. 2015). When moving upward and passing through the slab window, this magma will assimilate diamond and crustal minerals such as zircons, rutiles and monazites (Robinson et al. 2015; Zhou et al. 2014). Some zircons recovered from the PKO chromitite may also be recycled zircons in the asthenosphere or crystallized from chromitite-forming magmas (McGowan et al. 2015). Ophiolitic diamond and moissanite from Luobusa chromitite both have quite low but similar range of $\delta^{13}C$ values indicating that they may

Always consult and cite the final, published document. See http:/www.minsocam.org or GeoscienceWorld

have a similar organic carbon source from the subducting slab.

(c) Upwelling of the hot asthenosphere mantle provided extra heat to the overlying mantle wedge. Besides, with the addition of the slab-derived fluids into the mantle wedge, depleted mantle peridotite melted again and produced boninitic melts. Mixing of boninitic melts and silicon-rich magmas originated from the asthenosphere and reactions between melts and rocks result in the crystallization of large amounts of chromite below the Moho in the mantle wedge (Irvine 1977). At same time, both crustal and UHP minerals are enclosed in chromite grains.

ACKNOWLEDGEMENTS

We thank the Turkish geologists for assistance in the fieldwork, and the China National Research Center for the geochemical analyses. We appreciate Bin Shi from Chinese Academy of Geological Sciences for the SEM imaging and EDS analyses of these minerals. We would also like to thank Paul T. Robinson, Julian A. Pearce, Changqian Ma, Cong Zhang and Pengfei Zhang for their valuable suggestions in modifying this manuscript. Two reviewers, Sujoy Ghosh and Vincenzo Stagno, are greatly appreciated for their critical and constructive comments and suggestions which greatly improved the manuscript. We also thank Associate editor Mainak Mookherjee and Editor-in-Chief Keith Putirka for their scientific contributions and handling of our paper. This research was funded by grants from the Ministry of Science and Technology of China (2014DFR21270), China Geological Survey (121201102000150069, 12120115027201, and 201511022), the International Geoscience Programme (IGCP-649) and the Fund from the State Key Laboratory of Continental Tectonics and Dynamics (Z1301 -a20) and (Z1301 -a22).

REFERENCES CITED

Akbulut, M., González-Jiménez, J.M., Griffin, W.L., Belousova, E., O Reilly, S.Y., McGowan, N.and

This is a preprint, the final version is subject to change, of the American Mineralogist (MSA)
Cite as Authors (Year) Title. American Mineralogist, in press.
(DOI will not work until issue is live.) DOI: http://dx.doi.org/10.2138/am-2017-5850

Pearson, N.J. (2016) Tracing ancient events in the lithospheric mantle: A case study from ophiolitic chromitites of SW Turkey. Journal of Asian Earth Sciences, 119, 1-19.

Akmaz, R.M., Uysal, I.and Saka, S. (2014) Compositional variations of chromite and solid inclusions in ophiolitic chromitites from the southeastern Turkey: Implications for chromitite genesis. Ore Geology Reviews, 58, 208-224.

Alexander, C.O. (1993) Presolar SiC in chondrites: How variable and how many sources? Geochimica et cosmochimica acta, 57(12), 2869-2888.

Arai, S. (1994) Characterization of spinel peridotites by olivine-spinel compositional relationships: review and interpretation. Chemical geology, 113(3), 191-204.

Arai, S. (1997) Origin of podiform chromitites. Journal of Asian Earth Sciences, 15(2), 303-310.

Arai, S., Uesugi, J.and Ahmed, A.H. (2004) Upper crustal podiform chromitite from the northern Oman ophiolite as the stratigraphically shallowest chromitite in ophiolite and its implication for Cr concentration. Contributions to Mineralogy and Petrology, 147(2), 145-154.

Arai, S.and Matsukage, K. (1998) Petrology of a chromitite micropod from Hess Deep, equatorial Pacific: a comparison between abyssal and alpine-type podiform chromitites. Lithos, 43(1), 1-14.

Bonatti, E., Peyve, A., Kepezhinskas, P., Kurentsova, N., Seyler, M., Skolotnev, S.and Udintsev, G. (1992) Upper mantle heterogeneity below the Mid‐Atlantic Ridge, 0–15 N. Journal of Geophysical Research: Solid Earth, 97(B4), 4461-4476.

Bostock, M.G., Hyndman, R.D., Rondenay, S.and Peacock, S.M. (2002) An inverted continental Moho and serpentinization of the forearc mantle. Nature, 417(6888), 536-538.

Brunelli, D., Seyler, M., Cipriani, A., Ottolini, L.and Bonatti, E. (2006) Discontinuous melt extraction and weak refertilization of mantle peridotites at the Vema lithospheric section (Mid-Atlantic

Always consult and cite the final, published document. See http:/www.minsocam.org or GeoscienceWorld

This is a preprint, the final version is subject to change, of the American Mineralogist (MSA)
Cite as Authors (Year) Title. American Mineralogist, in press.
(DOI will not work until issue is live.) DOI: http://dx.doi.org/10.2138/am-2017-5850

Ridge). Journal of Petrology, 47(4), 745-771.

Caran, Ş., Çoban, H., Flower, M.F., Ottley, C.J.and Yılmaz, K. (2010) Podiform chromitites and mantle peridotites of the Antalya ophiolite, Isparta Angle (SW Turkey): implications for partial melting and melt–rock interaction in oceanic and subduction-related settings. Lithos, 114(3), 307-326.

Cartigny, P. (2005) Stable isotopes and the origin of diamond. Elements, 1(2), 79-84.

Çelik, Ö.F., Michel, D.and Gilbert, F. (2006) Precise 40 Ar–39 Ar ages from the metamorphic sole rocks of the Tauride Belt Ophiolites, southern Turkey: implications for the rapid cooling history. Geological Magazine, 02(143), 213-227.

Dickey, J.S. (1975) A hypothesis of origin for podiform chromite deposits. Geochimica Et Cosmochimica Acta, 39(6), 1061−1074.

Dilek, Y., Thy, P., Hacker, B.and Grundvig, S. (1999) Structure and petrology of Tauride ophiolites and mafic dike intrusions (Turkey): Implications for the Neotethyan ocean. Geological Society of America Bulletin, 111(8), 1192-1216.

Dilek, Y.and Furnes, H. (2011) Ophiolite genesis and global tectonics: Geochemical and tectonic fingerprinting of ancient oceanic lithosphere. Geological Society of America Bulletin, 123(3/4), 387-411.

Frost, D.J. (2008) The upper mantle and transition zone. Elements, 4(3), 171-176.

Frost, D.J.and McCammon, C.A. (2008) The redox state of Earth's mantle. Annual Review of Earth and Planetary Sciences, 36, 389-420.

Ghosh, S., Ohtani, E., Litasov, K.D., Suzuki, A., Dobson, D.and Funakoshi, K. (2013) Effect of water in depleted mantle on post-spinel transition and implication for 660km seismic discontinuity.

Always consult and cite the final, published document. See http:/www.minsocam.org or GeoscienceWorld

Earth and Planetary Science Letters, 371, 103-111.

Golubkova, A., Schmidt, M.W.and Connolly, J.A.D. (2016) Ultra-reducing conditions in average mantle peridotites and in podiform chromitites: a thermodynamic model for moissanite (SiC) formation. Contributions to Mineralogy & Petrology, 171(5), 1-17.

González-Jiménez, J.M., Griffin, W.L., Proenza, J.A., Gervilla, F., O'Reilly, S.Y., Akbulut, M., Pearson, N.J.and Arai, S. (2014) Chromitites in ophiolites: How, where, when, why? Part II. The crystallization of chromitites. Lithos, 189(2014), 140-158.

González-Jiménez, J.M., Proenza, J.A., Gervilla, F., Melgarejo, J.C., Blanco-Moreno, J.A., Ruiz-Sánchez, R.and Griffin, W.L. (2011) High-Cr and high-Al chromitites from the Sagua de Tánamo district, Mayarí-Cristal Ophiolitic Massif (eastern Cuba): constraints on their origin from mineralogy and geochemistry of chromian spinel and platinum-group elements. Lithos, 125(1), 101-121.

Griffin, W.L., Afonso, J.C., Belousova, E.A., Gain, S.E., Gong, X., González-Jiménez, J.M., Howell, D., Huang, J., McGowan, N.and Pearson, N.J. (2016) Mantle Recycling: Transition Zone Metamorphism of Tibetan Ophiolitic Peridotites and its Tectonic Implications. Journal of Petrology,2016, 1-30.

Hellebrand, E., Snow, J.E., Hoppe, P.and Hogmann, A.W. (2002) Garnet-field melting and late-stage refertilization in ‘residual’ abyssal peridotites from the Central Indian Ridge. Journal of Petrology, 43(12), 2305-2338.

Howell, D., Griffin, W.L., Yang, J., Gain, S., Stern, R.A., Huang, J., Jacob, D.E., Xu, X., Stokes, A.J.and O'Reilly, S.Y. (2015) Diamonds in ophiolites: Contamination or a new diamond growth environment? Earth and Planetary Science Letters, 430, 284-295.

Always consult and cite the final, published document. See http:/www.minsocam.org or GeoscienceWorld

Irvine, T.N. (1977) Origin of chromitite layers in the Muskox intrusion and other stratiform intrusions: a new interpretation. Geology, 5(5), 273-277.

Ishii, T. (1992) Petrological studies of peridotites from diapiric serpentinite seamounts in the Izu-Ogasawara-Mariana forearc, LEG125. Proc. ODP, Sci. Results, 125, 445-485.

Jacob, D.E., Kronz, A.and Viljoen, K.S. (2004) Cohenite, native iron and troilite inclusions in garnets from polycrystalline diamond aggregates. Contributions to Mineralogy and Petrology, 146(5), 566-576.

Johnson, K.and Dick, H.J. (1992) Open system melting and temporal and spatial variation of peridotite and basalt at the Atlantis II fracture zone. Journal of Geophysical Research: Solid Earth, 97(B6), 9219-9241.

Kaminsky, F.V., Khachatryan, G.K., Andreazza, P., Araujo, D.and Griffin, W.L. (2009) Super-deep diamonds from kimberlites in the Juina area, Mato Grosso State, Brazil. Lithos, 112, 833-842.

Komor, S.C., Grove, T.L.and Hébert, R. (1990) Abyssal peridotites from ODP Hole 670A (21 10'N, 45 02'W): residues of mantle melting exposed by non-constructive axial divergence. Proceedings of Ocean Drilling Program, Scientific Results, 109, 85-101.

Leung, I., Guo, W., Friedman, I.and Gleason, J. (1990) Natural occurrence of silicon carbide in a diamondiferous kimberlite from Fuxian. Nature, 346, 352-354.

Liang, F., Xu, Z.and Zhao, J. (2014) In‐situ Moissanite in Dunite: Deep Mantle Origin of Mantle Peridotite in Luobusa Ophiolite, Tibet. Acta Geologica Sinica (English Edition), 88(2), 517-529.

Lytwyn, J.N.and Casey, J.F. (1995) The geochemistry of postkinematic mafic dike swarms and subophiolitic metabasites, Pozanti-Karsanti ophiolite, Turkey: Evidence for ridge subduction. Geological Society of America Bulletin, 107(7), 830-850.

Always consult and cite the final, published document. See http:/www.minsocam.org or GeoscienceWorld

This is a preprint, the final version is subject to change, of the American Mineralogist (MSA)
Cite as Authors (Year) Title. American Mineralogist, in press.
(DOI will not work until issue is live.) DOI: http://dx.doi.org/10.2138/am-2017-5850

Mathez, E.A., Fogel, R.A., Hutcheon, I.D.and Marshintsev, V.K. (1995) Carbon isotopic composition and origin of SiC from kimberlites of Yakutia, Russia. Geochimica et Cosmochimica Acta, 59(4), 781-791.

McGowan, N.M., Griffin, W.L., González-Jiménez, J.M., Belousova, E., Afonso, J.C., Shi, R., McCammon, C.A., Pearson, N.J.and O Reilly, S.Y. (2015) Tibetan chromitites: Excavating the slab graveyard. Geology, 43(2), 179-182.

Moissan, H.and Siemens, F. (1904) Sur la Solubilité du Silicium dans le Zinc et dans le Plomb. CR Acad. Sci. Paris, 139, 773-780.

Moix, P., Beccaletto, L., Kozur, H.W., Hochard, C., Rosselet, F.and Stampfli, G.M. (2008) A new classification of the Turkish terranes and sutures and its implication for the paleotectonic history of the region. Tectonophysics, 451(1), 7-39.

Niida, K. (1997) 12, Mineralogy of Mark peridotites: replacement through magma chaneling examined from Hole 920D, Mark area. Proceedings of Ocean Drilling Program, Scientific Results, 153, 265-275

Okamura, H., Arai, S.and Kim, Y. (2006) Petrology of forearc peridotite from the Hahajima Seamount, the Izu-Bonin arc, with special reference to chemical characteristics of chromian spinel. Mineralogical Magazine, 70(1), 15-26.

Pagé, P.and Barnes, S. (2009) Using trace elements in chromites to constrain the origin of podiform chromitites in the Thetford Mines ophiolite, Québec, Canada. Economic Geology, 104(7), 997-1018.

Parkinson, I.J.and Pearce, J.A. (1998) Peridotites from the Izu – Bonin – Mariana forearc (ODP Leg 125): evidence for mantle melting and melt – mantle interaction in a supra-subduction zone

Always consult and cite the final, published document. See http:/www.minsocam.org or GeoscienceWorld

setting. Journal of Petrology, 39(9), 1577-1618.

Parlak, O., HÖck, V.and Delaloye, M. (2000) Suprasubduction zone origin of the Pozanti-Karsanti ophiolite (southern Turkey) deduced from whole-rock and mineral chemistry of the gabbroic cumulates. Geological Society, London, Special Publications, 173(1), 219-234.

Parlak, O., Höck, V.and Delaloye, M. (2002) The supra-subduction zone Pozanti – Karsanti ophiolite, southern Turkey: evidence for high-pressure crystal fractionation of ultramafic cumulates. Lithos, 65(1), 205-224.

Pearce, J.A. (2014) Immobile element fingerprinting of ophiolites. Elements, 10(2), 101-108.

Polat, A., Casey, J.F.and Kerrich, R. (1996) Geochemical characteristics of accreted material beneath the Pozanti-Karsanti ophiolite, Turkey: Intra-oceanic detachment, assembly and obduction. Tectonophysics, 263(1), 249-276.

Polat, A.and Casey, J.F. (1995) A structural record of the emplacement of the Pozanti-Karsanti ophiolite onto the Menderes-Taurus block in the late Cretaceous, eastern Taurides, Turkey. Journal of Structural Geology, 17(12), 1673-1688.

Ringwood, A.E. (1975) Composition and Petrology of the Earth's Mantle. 618 p. McGraw-Hill, New York.

Robinson, P.T., Bai, W., Malpas, J., Yang, J., Zhou, M., Fang, Q., Hu, X., Cameron, S.and Staudigel, H. (2004) Ultra-high pressure minerals in the Luobusa Ophiolite, Tibet, and their tectonic implications. Special Publication-Geological Society of London, 226, 247-272.

Robinson, P.T., Trumbull, R.B., Schmitt, A., Yang, J., Li, J., Zhou, M., Erzinger, J., Dare, S.and Xiong, F. (2015) The origin and significance of crustal minerals in ophiolitic chromitites and peridotites. Gondwana Research, 27(2), 486-506.

Always consult and cite the final, published document. See http:/www.minsocam.org or GeoscienceWorld

Rollinson, H.and Adetunji, J. (2015) The geochemistry and oxidation state of podiform chromitites from the mantle section of the Oman ophiolite: a review. Gondwana Research, 27(2), 543-554.

Saka, S., Uysal, I., Akmaz, R.M., Kaliwoda, M.and Hochleitner, R. (2014) The effects of partial melting, melt – mantle interaction and fractionation on ophiolite generation: Constraints from the late Cretaceous Pozantı-Karsantı ophiolite, southern Turkey. Lithos, 2014 (202), 300-316.

Schmidt, M.W., Gao, C., Golubkova, A., Rohrbach, A.and Connolly, J.A. (2014) Natural moissanite (SiC) – a low temperature mineral formed from highly fractionated ultra-reducing COH-fluids. Progress in Earth and Planetary Science, 1(1), 1-14.

Seyler, M., Cannat, M.and Mével, C. (2003) Evidence for major - element heterogeneity in the mantle source of abyssal peridotites from the Southwest Indian Ridge (52 to 68 E). Geochemistry, Geophysics, Geosystems, 4(2), 1-33.

Shirey, S.B., Cartigny, P., Frost, D.J., Keshav, S., Nestola, F., Nimis, P., Pearson, D.G., Sobolev, N.V.and Walter, M.J. (2013) Diamonds and the geology of mantle carbon. Reviews in Mineralogy & Geochemistry, 75(1), 355-421.

Shiryaev, A.A., Griffin, W.L.and Stoyanov, E. (2011) Moissanite (SiC) from kimberlites: polytypes, trace elements, inclusions and speculations on origin. Lithos, 122(3), 152-164.

Snow, J.E.and Dick, H.J. (1995) Pervasive magnesium loss by marine weathering of peridotite. Geochimica et Cosmochimica Acta, 59(20), 4219-4235.

Stachel, T., Brey, G.P.and Harris, J.W. (2005) Inclusions in sublithospheric diamonds: glimpses of deep Earth. Elements, 1(2), 73-78.

Stachel, T.and Luth, R.W. (2015) Diamond formation—Where, when and how? Lithos, 220, 200-220.

Stagno, V., Frost, D.J., McCammon, C.A., Mohseni, H.and Fei, Y. (2015) The oxygen fugacity at

This is a preprint, the final version is subject to change, of the American Mineralogist (MSA)
Cite as Authors (Year) Title. American Mineralogist, in press.
(DOI will not work until issue is live.) DOI: http://dx.doi.org/10.2138/am-2017-5850

which graphite or diamond forms from carbonate-bearing melts in eclogitic rocks. Contributions to Mineralogy and Petrology, 169(2), 1-18.

Stagno, V., Ojwang, D.O., McCammon, C.A.and Frost, D.J. (2013) The oxidation state of the mantle and the extraction of carbon from Earth/'s interior. Nature, 493(7430), 84-88.

Stagno, V.and Frost, D.J. (2010) Carbon speciation in the asthenosphere: Experimental measurements of the redox conditions at which carbonate-bearing melts coexist with graphite or diamond in peridotite assemblages. Earth and Planetary Science Letters, 300(1), 72-84.

Stephens, C.J. (1997) Heterogeneity of oceanic peridotite from the western canyon wall at MARK: results from site 920. Proceedings of the Ocean Drilling Program, Scientific results, 153, 285-303.

Stern, R.J. (2004) Subduction initiation: spontaneous and induced. Earth and Planetary Science Letters, 226(3), 275-292.

Stern, R.J., Reagan, M., Ishizuka, O., Ohara, Y.and Whattam, S. (2012) To understand subduction initiation, study forearc crust: To understand forearc crust, study ophiolites. Lithosphere, 4(6), 469-483.

Stevens, R.E. (1944) Composition of some chromites of the western hemisphere. American Mineralogist, 29(1-2), 1-34.

Tekeli, O., Aksay, A., Urgun, B.M.and Isik, A. (1983) Geology of the Aladag mountains. The Geology of the Taurus Belt. MTA Publications, Ankara, 143-158.

Thayer, T.P. (1964) Principal features and origin of podiform chromite deposits, and some observations on the Guelman-Soridag District, Turkey. Economic Geology, 59(8), 1497-1524.

Thayer, T.P. (1970) Chromite segregations as petrogenetic indicators. Special Publication - Geological Society of South Africa, 1, 380-390.

Always consult and cite the final, published document. See http:/www.minsocam.org or GeoscienceWorld

Thuizat, R., Whitechurch, H., Montigny, R.and Juteau, T. (1981) K-Ar dating of some infra-ophiolitic metamorphic soles from the Eastern Mediterranean: new evidence for oceanic thrustings before obduction. Earth and Planetary Science Letters, 52(2), 302-310.

Tian, Y., Yang, J., Robinson, P.T., Xiong, F., Yuan, L.I., Zhang, Z., Liu, Z., Liu, F.and Niu, X. (2015) Diamond Discovered in High-Al Chromitites of the Sartohay Ophiolite,Xinjiang Province,China. Acta Geologica Sinica, 89(2), 332-340.

Trumbull, R.B., Yang, J., Robinson, P.T., Di Pierro, S., Vennemann, T.and Wiedenbeck, M. (2009) The carbon isotope composition of natural SiC (moissanite) from the Earth's mantle: New discoveries from ophiolites. Geochmica Et Cosmochimica Acta, 113(3), 612-620.

Ucurum, A., Koptagel, O.and Lechler, P.J. (2006) Main-component geochemistry and Platinum-Group-Element potential of Turkish chromite deposits, with emphasis on the Mugla area. International Geology Review, 48(3), 241-254.

Ueda, K., Gerya, T.and Sobolev, S.V. (2008) Subduction initiation by thermal chemical plumes: Numerical studies. Physics of the Earth & Planetary Interiors, 171(1), 296-312.

Ulmer, G.C., Grandstaff, D.E., Woermann, E., Göbbels, M., Schönitz, M.and Woodland, A.B. (1998) The redox stability of moissanite (SiC) compared with metal-metal oxide buffers at 1773 K and at pressures up to 90 kbar. Neues Jahrbuch für Mineralogie-Abhandlungen, 172(2), 279-307.

Uysal, I., Tarkian, M., Sadiklar, M.B., Zaccarini, F., Meisel, T., Garuti, G.and Heidrich, S. (2009) Petrology of Al-and Cr-rich ophiolitic chromitites from the Muğla, SW Turkey: implications from composition of chromite, solid inclusions of platinum-group mineral, silicate, and base-metal mineral, and Os-isotope geochemistry. Contributions to Mineralogy and Petrology, 158(5), 659-674.

Always consult and cite the final, published document. See http:/www.minsocam.org or GeoscienceWorld

Uysal, İ., Tarkian, M., Sadiklar, M.B., Zaccarini, F., Meisel, T., Garuti, G.and Heidrich, S. (2009) Petrology of Al-and Cr-rich ophiolitic chromitites from the Muğla, SW Turkey: implications from composition of chromite, solid inclusions of platinum-group mineral, silicate, and base-metal mineral, and Os-isotope geochemistry. Contributions to Mineralogy and Petrology, 158(5), 659-674.

Uysal, I., Zaccarini, F., Garuti, G., Meisel, T., Tarkian, M., Bernhardt, H.J.and Sadiklar, M.B. (2007) Ophiolitic chromitites from the Kahramanmaras area, southeastern Turkey: their platinum group elements (PGE) geochemistry, mineralogy and Os-isotope signature. Ofioliti, 32, 151-161.

Whattam, S.A.and Stern, R.J. (2011) The ‘subduction initiation rule’: a key for linking ophiolites, intra-oceanic forearcs, and subduction initiation. Contributions to Mineralogy and Petrology, 162(5), 1031-1045.

Xiong, F., Yang, J., Robinson, P.T., Xu, X., Liu, Z., Li, Y., Li, J.and Chen, S. (2015) Origin of podiform chromitite, a new model based on the Luobusa ophiolite, Tibet. Gondwana Research, 27(2), 525-542.

Xu, S., Wu, W., Xiao, W., Yang, J., Chen, J., Ji, S.and Liu, Y. (2008) Moissanite in serpentinite from the Dabie Mountains in China. Mineralogical Magazine, 72(4), 899-908.

Xu, X., Yang, J., Robinson, P.T., Xiong, F., Ba, D.and Guo, G. (2015) Origin of ultrahigh pressure and highly reduced minerals in podiform chromitites and associated mantle peridotites of the Luobusa ophiolite, Tibet. Gondwana Research, 27(2), 686-700.

Yamamoto, S., Komiya, T., Hirose, K.and Maruyama, S. (2009) Coesite and clinopyroxene exsolution lamellae in chromites: In-situ ultrahigh-pressure evidence from podiform chromitites in the Luobusa ophiolite, southern Tibet. Lithos, 109(3), 314-322.

Always consult and cite the final, published document. See http:/www.minsocam.org or GeoscienceWorld

This is a preprint, the final version is subject to change, of the American Mineralogist (MSA)
Cite as Authors (Year) Title. American Mineralogist, in press.
(DOI will not work until issue is live.) DOI: http://dx.doi.org/10.2138/am-2017-5850

Yamamoto, S., Komiya, T., Yamamoto, H., Kaneko, Y., Terabayashi, M., Katayama, I., Iizuka, T., Maruyama, S., Yang, J.and Kon, Y. (2013) Recycled crustal zircons from podiform chromitites in the Luobusa ophiolite, southern Tibet. Island Arc, 22(1), 89-103.

Yang, J., Dobrzhinetskaya, L., Bai, W., Fang, Q., Robinson, P.T., Zhang, J.and Green, H.W. (2007) Diamond-and coesite-bearing chromitites from the Luobusa ophiolite, Tibet. Geology, 35(10), 875-878.

Yang, J., Meng, F., Xu, X., Robinson, P.T., Dilek, Y., Makeyev, A.B., Wirth, R., Wiedenbeck, M.and Cliff, J. (2015) Diamonds, native elements and metal alloys from chromitites of the Ray-Iz ophiolite of the Polar Urals. Gondwana Research, 27(2), 459-485.

Yang, J., Robinson, P.T.and Dilek, Y. (2014) Diamonds in ophiolites. Elements, 10(2), 127-130.

Zhang, P., Uysal, I., Zhou, M., Su, B.and Avcı, E. (2016) Subduction initiation for the formation of high-Cr chromitites in the Kop ophiolite, NE Turkey. Lithos, 260, 345-355.

Zheng, J., Griffin, W.L., O'Reilly, S.Y., Zhang, M.and Pearson, N. (2006) Zircons in mantle xenoliths record the Triassic Yangtze–North China continental collision. Earth and Planetary Science Letters, 247(1), 130-142.

Zhou, M., Robinson, P.T., Malpas, J., Aitchison, J., Sun, M., Bai, W., Hu, X.and Yang, J. (2001) Melt/mantle interaction and melt evolution in the Sartohay high-Al chromite deposits of the Dalabute ophiolite (NW China). Journal of Asian Earth Sciences, 19(4), 517-534.

Zhou, M., Robinson, P.T., Malpas, J.and Li, Z. (1996) Podiform chromitites in the Luobusa ophiolite (southern Tibet): Implications for melt-rock interaction and chromite segregation in the upper mantle. Journal of Petrology, 37(1), 3-21.

Zhou, M., Robinson, P.T., Su, B., Gao, J., Li, J., Yang, J.and Malpas, J. (2014) Compositions of

Always consult and cite the final, published document. See http:/www.minsocam.org or GeoscienceWorld

This is a preprint, the final version is subject to change, of the American Mineralogist (MSA)
Cite as Authors (Year) Title. American Mineralogist, in press.
(DOI will not work until issue is live.) DOI: http://dx.doi.org/10.2138/am-2017-5850

chromite, associated minerals, and parental magmas of podiform chromite deposits: The role of slab contamination of asthenospheric melts in suprasubduction zone environments. Gondwana Research, 26(1), 262-283.

Zhou, M.F., Robinson, P.T., Su, B.X., Gao, J.F., Li, J.W., Yang, J.S.and Malpas, J. (2014) Compositions of chromite, associated minerals, and parental magmas of podiform chromite deposits: The role of slab contamination of asthenospheric melts in suprasubduction zone environments. Gondwana Research, 26(1), 262－283.

Zhou, M.F., Sun, M., Keays, R.R.and Kerrich, R.W. (1998) Controls on platinum-group elemental distributions of podiform chromitites: a case study of high-Cr and high-Al chromitites from Chinese orogenic belts. Geochimica et Cosmochimica Acta, 62(4), 677-688.

Zhu, H., Jingsui, Y., Robinson, P.T., Yongwang, Z., Fahui, X., Zhao, L., Zhongming, Z.and Wei, X. (2015) The Discovery of Diamonds in Chromitites of the Hegenshan Ophiolite, Inner Mongolia, China. Acta Geologica Sinica (English Edition), 89(2), 341-350.

Figure Captions

Fig. 1. Distribution of ophiolites and surrounding regions of Turkey, after Moix et al. (2008).

Fig. 2. Regional geological map of the PKO, modified after Polat and Casey (1995).

Fig. 3. Field photographs of different rock units of the PKO. (a) Dunite occurring as lenses or patches in harzburgite; (b) Chromite bands in cumulate dunite around the Moho; (c) Podiform chromitites hosted by strongly serpentinized harzburgite; (d) Podiform chromitite showing nodular texture.

Fig. 4. Photomicrograph of peridotites and podiform chromitites. (a) Harzburgites of the PKO; (b) Olivine enclosed in euhedral chromite; (c) Strongly serpentinized dunite; (d) massive chromitite with

Always consult and cite the final, published document. See http:/www.minsocam.org or GeoscienceWorld

euhedral silicate inclusion; (e) Olivine inclusion in chromitites; (f) Euhedral clinopyroxene inclusions in chromitite. Ol-Olivine; Opx-Orthopyroxene; Cpx-Clinopyroxene; Chr-chromite.

Fig 5. Compositional variations of olivine and chromite from harzburgites and podiform chromitites in the PKO. (a) Plot of chromite Cr# vs olivine Fo value for the harzburgites after Arai. (1994) and Pearce et al. (2000). OSMA-Olivine-spinel mantle array; SSZ-Suprasubduction zone; and FMM-Fertile MORB mantle; (b) Plot of PKO chromites on ternary major oxide (Fe_2O_3-Al_2O_3-Cr_2O_3) nomenclature diagram (after Stevens, 1944), 1 = aluminum magnetite, 2 = chrome magnetite, 3 = ferrichromite, 4 = aluminum chromite, 5 = chrome spinel, 6 = ferrispinel, grey field of Turkish chromites are from Ucurum et al. (2006); (c) Cr# vs. Mg#; (d) Cr# vs. TiO_2; (e) Al_2O_3 vs. Cr_2O_3; and (f) TiO_2 vs. Cr_2O_3 of chromites. Data for abyssal peridotites are from Bonatti et al. (1992); Brunelli et al. (2006); Hellebrand et al. (2002); Johnson and Dick (1992); Komor et al. (1990); Niida (1997); Seyler et al. (2003); Snow and Dick (1995); Stephens (1997); Data for forearc peridotites are from Ishii (1992); Okamura et al. (2006); Parkinson and Pearce (1998); Podiform, stratiform and crustal chromitite fields are from Arai et al. (2004).

Fig 6. Photographs of diamonds recovered from the PKO chromitite. (a) Microphotograph showing abundant light-yellow to yellow diamonds; (b) SEM image showing octahedral diamond; (c) Raman spectrogram showing typical Raman shift around 1332 cm^{-1}; (d) SEM image for rounded diamond.

Fig 7. Photographs of moissanite separated from podiform chromitite. (a) Microphotograph of moissanite in blue color; (b) SEM image for moissanite; (c) Typical Raman patterns of moissanite; (d) Microphotograph of moissanite in light-green to green color; (e) SEM image showing moissanite with polycrystalline; and (f) EDS analysis of moissanite.

Fig 8. Photographs for silicates of octahedral pseudomorph. (a) Microphotograph of octahedral silicates in different color; (b) SEM image of silicate showing perfect octahedral pseudomorph; (c) Octahedral silicate bonded to chromite; (d) surface characteristics of octahedral silicate; (e) and (f) EDS analytical results for different octahedral silicates.

Fig 9. Other minerals recovered from podiform chromitite. (a) Microphotograph of zircons in different morphologies and colors; (b) SEM image for rounded zircon; (c) Raman pattern for zircon from Pozanti-Karsanti chromitite; (d) Microphotograph of monazites; (e) SEM image of monazite; (f) Raman pattern for monazite; (g) Microphotograph of rutiles; (h) SEM image for rutile; and (i) Raman pattern for rutile.

Supplementary 1. Tectonostratigrapic section of the Aladag region, modified after Polat et al. (1996).

Supplementary 2. Photos of different chromitite types under the microscope. (a) Disseminated chromitites in the cumulate dunites; (b) Massive chromitites in the cumulate dunites; (c) Nodular chromitites in the harzburgites; (d) Massive chromitites in the harzburgites.

Supplementary 3. Representative electron probe microanalyses of minerals in the harzburgites and chromitites from the PKO.

Always consult and cite the final, published document. See http:/www.minsocam.org or GeoscienceWorld

This is a preprint, the final version is subject to change, of the American Mineralogist (MSA)
Cite as Authors (Year) Title. American Mineralogist, in press.
(DOI will not work until issue is live.) DOI: http://dx.doi.org/10.2138/am-2017-5850

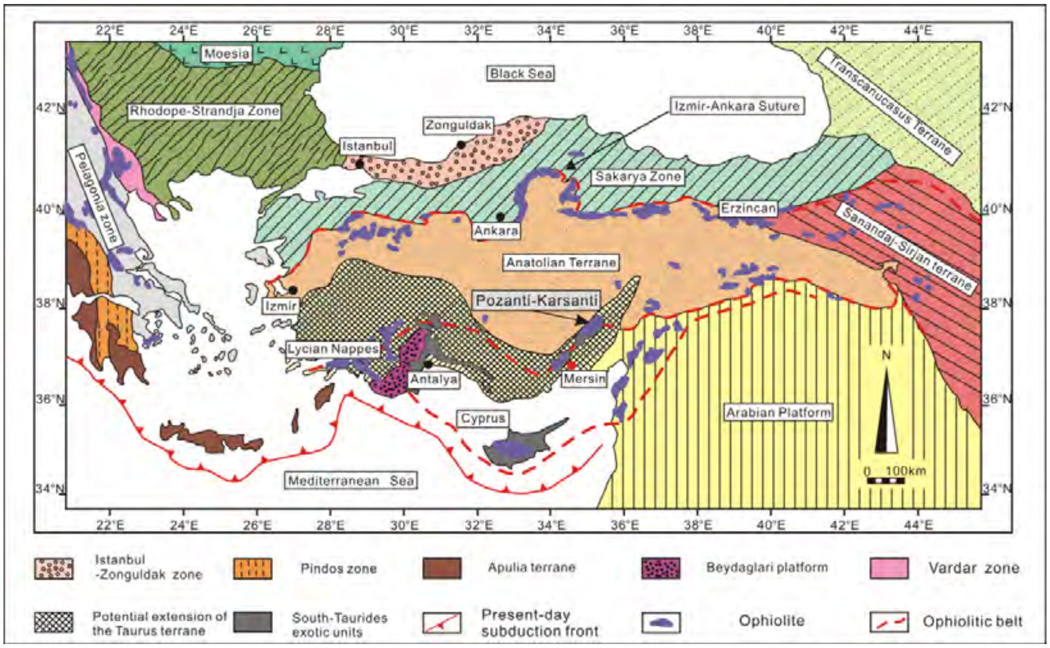

Fig. 1

Always consult and cite the final, published document. See http:/www.minsocam.org or GeoscienceWorld

This is a preprint, the final version is subject to change, of the American Mineralogist (MSA)
Cite as Authors (Year) Title. American Mineralogist, in press.
(DOI will not work until issue is live.) DOI: http://dx.doi.org/10.2138/am-2017-5850

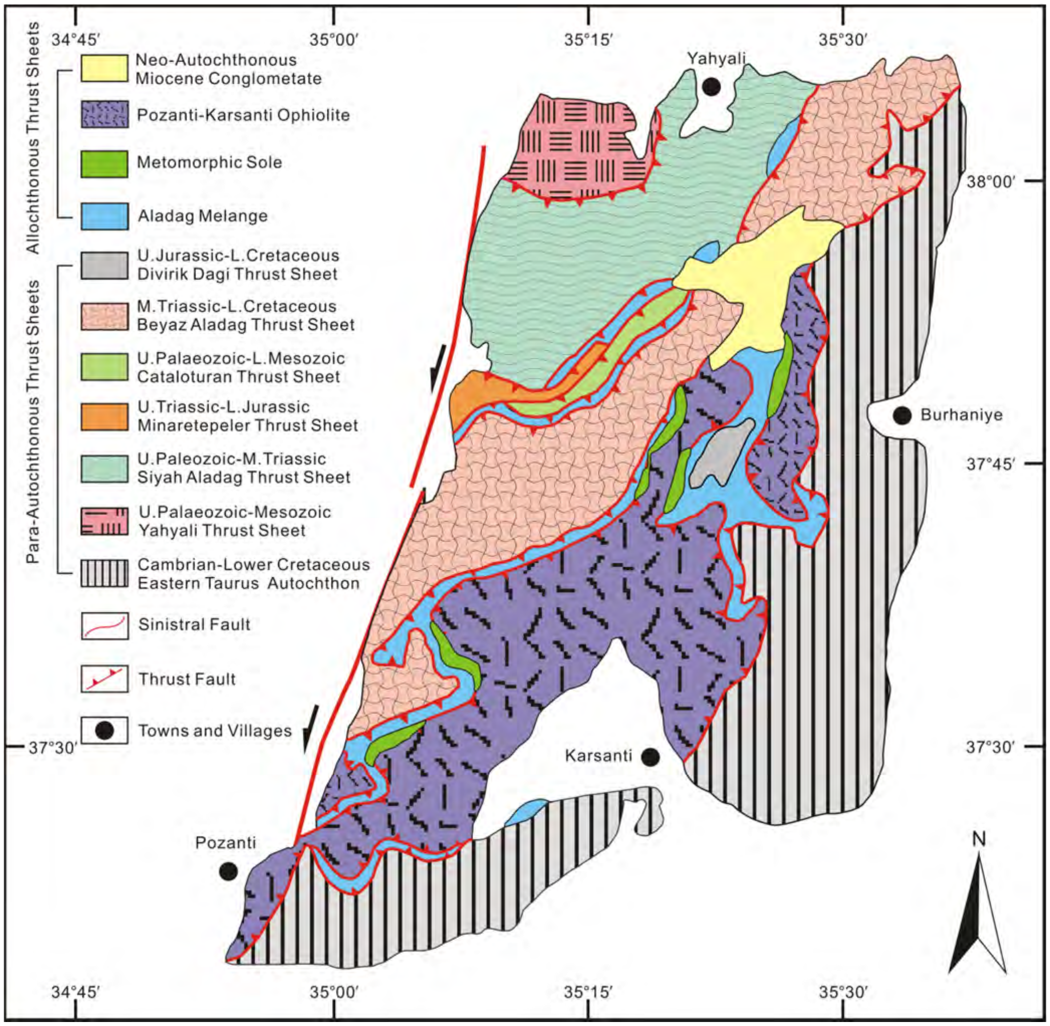

Fig. 2

Always consult and cite the final, published document. See http:/www.minsocam.org or GeoscienceWorld

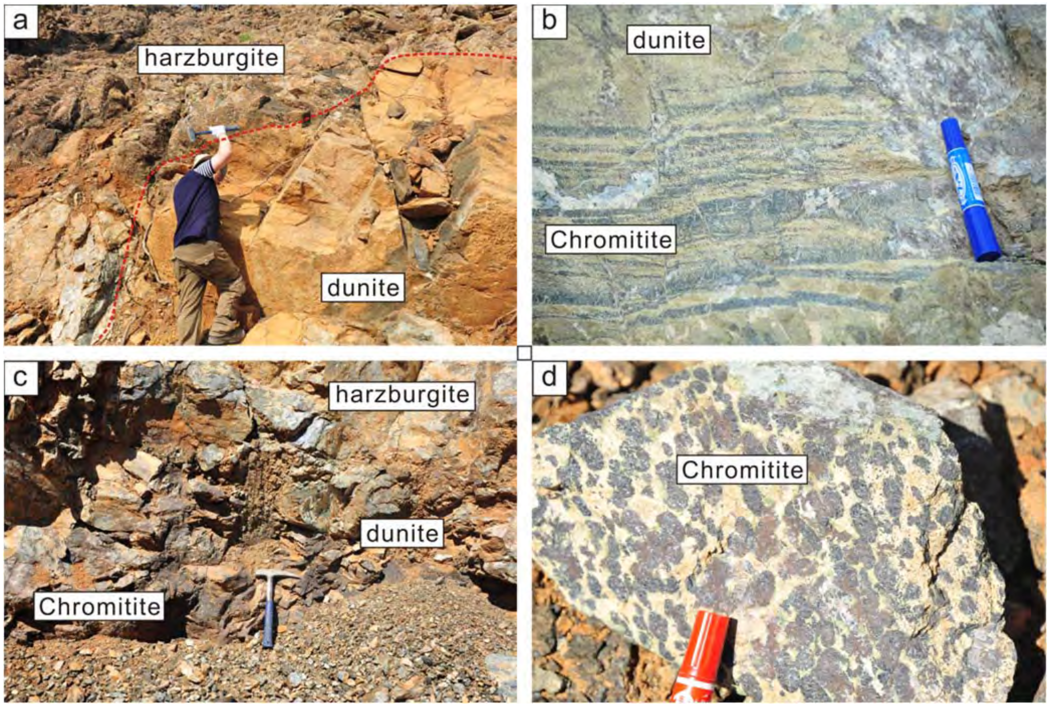

Fig. 3

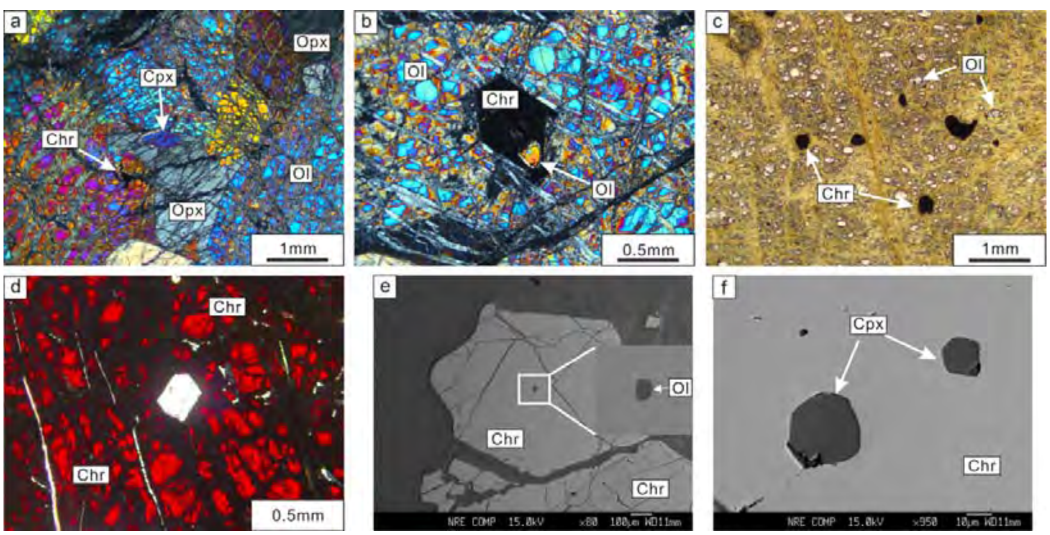

Fig. 4

Always consult and cite the final, published document. See http:/www.minsocam.org or GeoscienceWorld

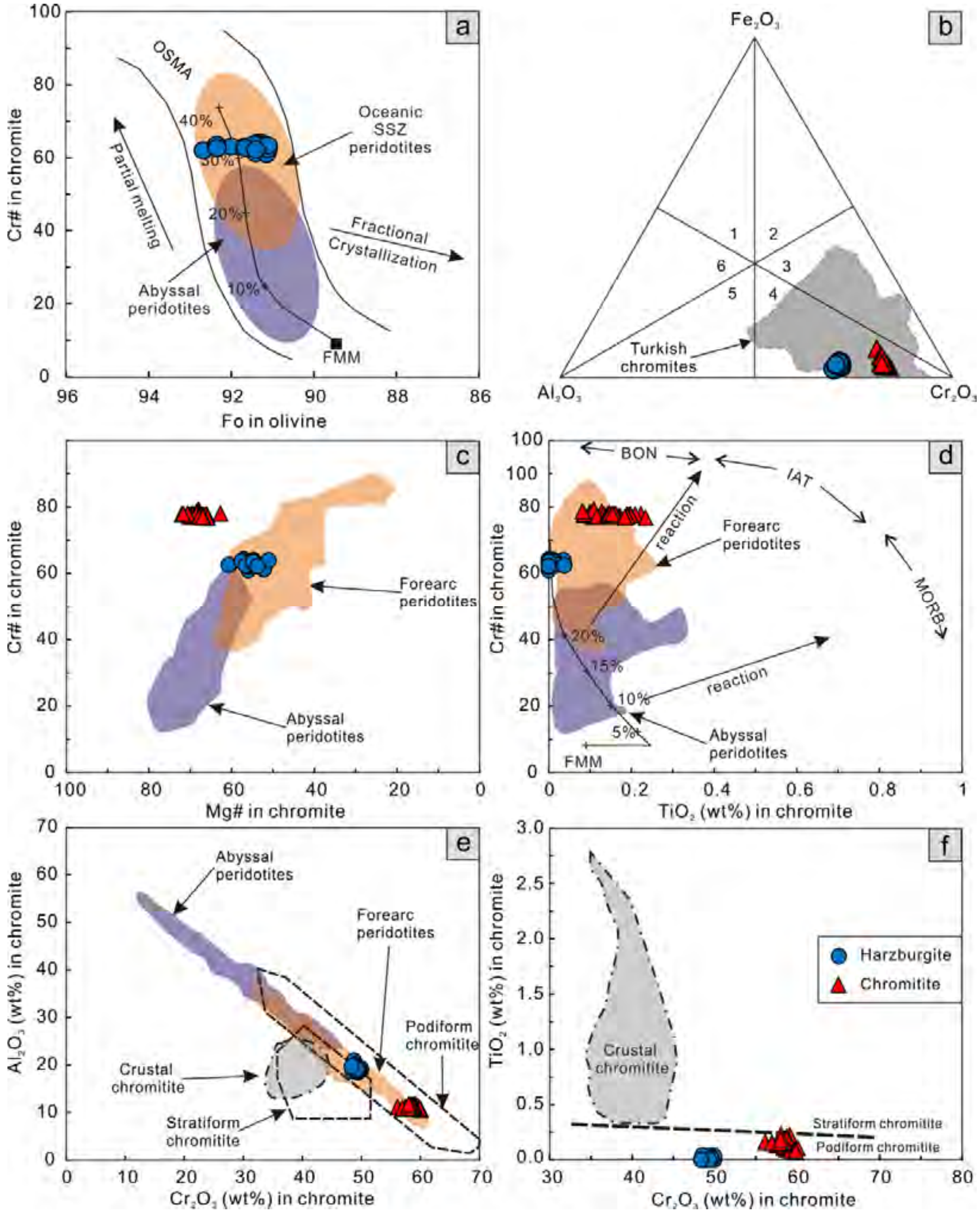

Fig.5

Always consult and cite the final, published document. See http:/www.minsocam.org or GeoscienceWorld

This is a preprint, the final version is subject to change, of the American Mineralogist (MSA)
Cite as Authors (Year) Title. American Mineralogist, in press.
(DOI will not work until issue is live.) DOI: http://dx.doi.org/10.2138/am-2017-5850

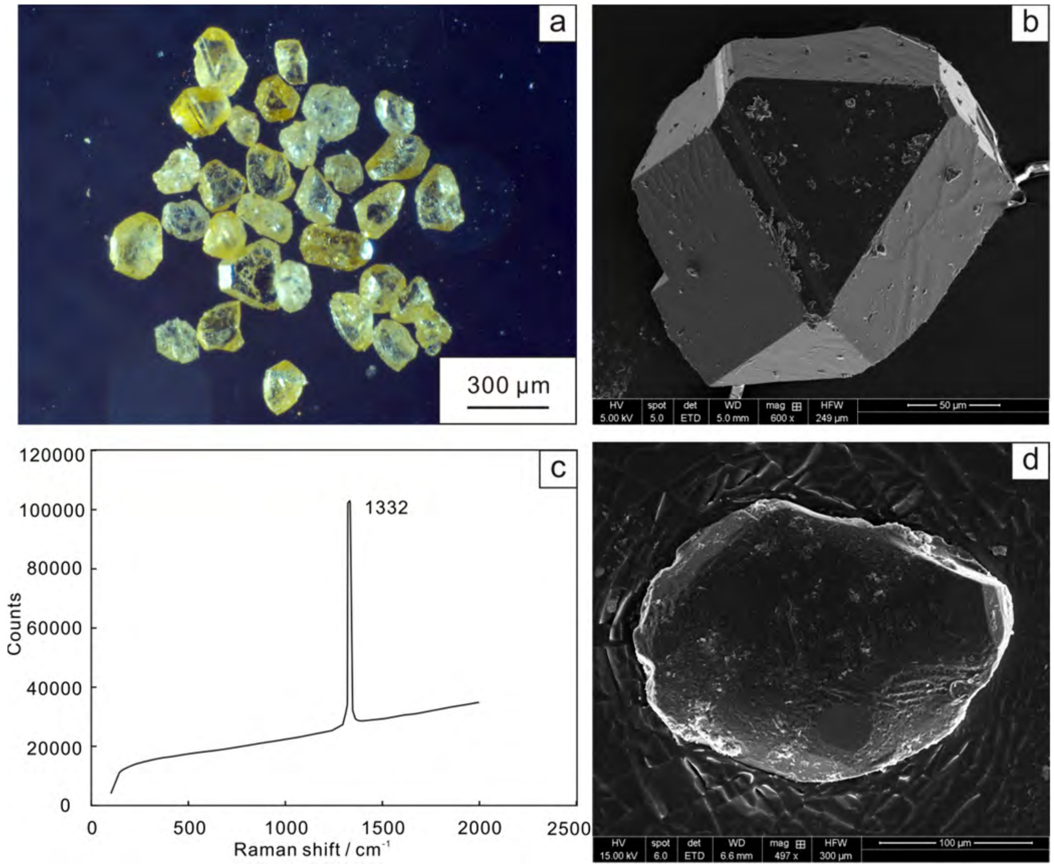

Fig. 6

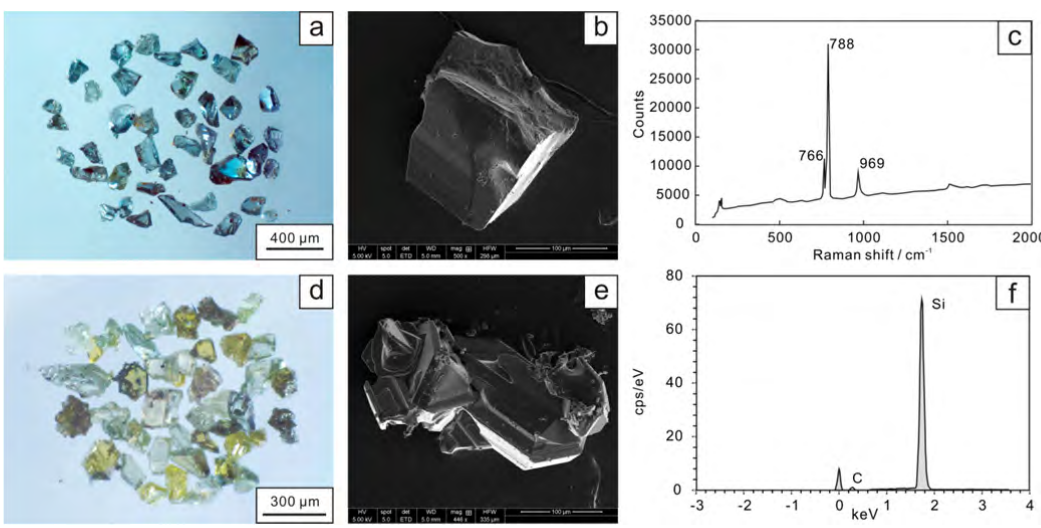

Fig. 7

Always consult and cite the final, published document. See http:/www.minsocam.org or GeoscienceWorld

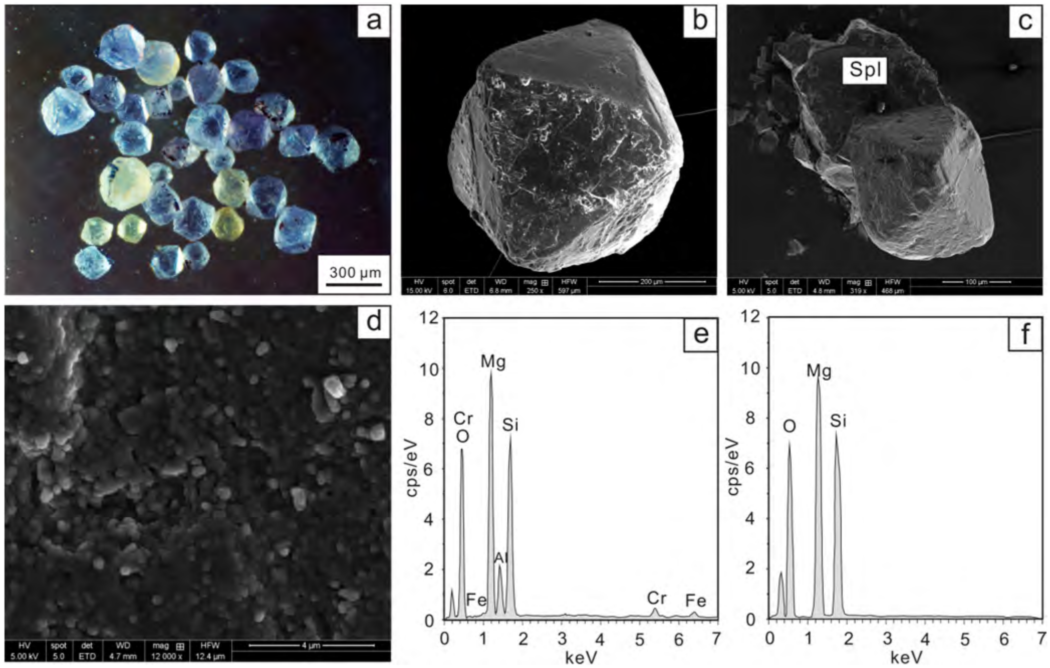

Fig. 8

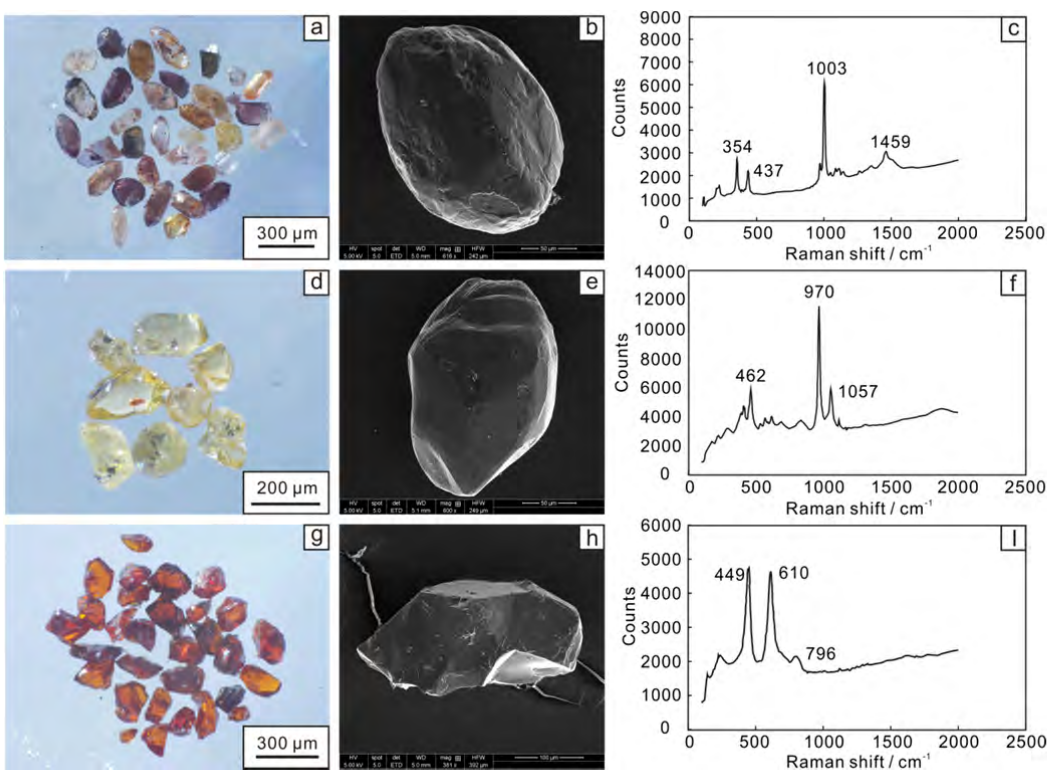

Fig. 9

Always consult and cite the final, published document. See http:/www.minsocam.org or GeoscienceWorld